# Free Solution Assay Signal Modulation in Variable-Stem-Length Hairpin Aptamers

Michael N. Kammer[1], Amanda K. Kussrow[1], Ian R. Olmsted[1], George W. Jackson[2] and Darryl J. Bornhop[1*]

[1]Vanderbilt Department of Chemistry; [2]Base Pair Biotechnologies, Inc. Pearland, TX 77584

**ABSTRACT:** Interferometric measurements of Free Solution Assays (FSAs) quantify changes in molecular conformation and hydration upon binding. Here we demonstrate that aptamer probes designed to undergo varying levels of conformational change upon binding produce corresponding variations in FSA signals. A series of hairpin aptamers were synthesized for the small molecule (tenofovir) with identical loop regions that contain the binding pocket, with between 2 and 10 self-associating base pairings in the stem region. Aptamers selected for tenofovir showed a decrease in FSA signal and binding affinity (increase in $K_D$) with increasing stem length. Thermodynamic calculations of the Gibbs free energy ($\Delta G$) reported a decrease in $\Delta G$ with respect to a corresponding increase in aptamer stem length. Collectively these observations provide an expanded understanding of FSA and demonstrate the potential for rational design of label-free aptamer beacons using FSA as readout.

**Introduction**

The Free Solution Assay (FSA) is a label-free, solution-phase methodology that enables characterization of molecular interactions for a broad range of species, rapidly, and in complex matrices.[1] The FSA method capitalizes upon changes in the solution dipole moment upon binding, which is measured using a compensated interferometric reader (CIR).[2] Because the FSA signal is a product of inherent properties of the binding interaction, there is no need for surface-immobilization or labeling of one of the interacting species.

The FSA signal arises from changes in molecular conformation and hydration upon binding, as described by the Free Solution Response Function (FreeSRF) given in Equation 1:

$$\rho = x\beta C$$

which states that the observed interferometric signal ($\rho$) is a function of the magnitude of conformation and hydration change upon binding, molar refractivity ($\chi$), the instrument response function ($\beta$), and the concentration of binding events (C).[3] Using quality structural information about the binding system, such as x-ray crystal structures of the unbound constituents and bound product, the magnitude of conformation and hydration changes can be calculated, allowing estimation of the binding signal.

An advantageous family of probe molecules for FSAs are aptamers, short segments of single-strand DNA or RNA molecules that can be rapidly and inexpensively designed to bind to a wide range of targets.[4] Aptamers provide inexpensive production, no cold-chain requirement, high affinity binding to their target, and excellent specificity to a desired target molecule, proving to be an attractive alternative to antibodies for many applications. Once identified, aptamers can be produced by purely synthetic means, requiring no organisms, cell culture or biological expression system. Therefore, aptamer reagents exhibit minimized lot-to-lot variability. Further, facile modifications can be made to aptamers during synthesis that can confer nuclease stability of the molecules in serum for *in vivo* and diagnostic applications.

Due to their ability to form a variety of three-dimensional structures, such as helices and single-stranded loops, aptamers can bind to diverse targets in a wide range of situations. They can serve as sensors,[4] therapeutics,[5] cellular process regulators,[6] and drug targeting guides.[7] Aptamers are also unique because they can be selected to bind, manipulate, inhibit, control, or detect small molecules in the complex matrix which will be used for the assay.[8]

Recently, there has been a renewed interest in the design of aptamers that bind small molecules due to the inherent limitations encountered when attempting to prepare small-molecule specific antibodies.[9] Small molecules can be highly bioactive compounds and include harmful toxins, beneficial drugs, antibiotics, nutrients, and serve as intercellular signal mediators or neurotransmitters. Numerous approaches to aptamer-based biosensing have been reported, including electrochemical,[10] colorimetric,[11] SERS,[12] refractive index (RI) detection,[13] and others.[14] These techniques all exhibit advantages and limitations, but aptamer-based biosensors, particularly the label-free strategies based on SPR and BLI that require immobilization, are complicated by chemical assembly, and are limited by background and surface fowling when attempting to make determinations at high sensitivity. Yet, aptamer-based FSAs have been recently shown useful for the high sensitivity measurement of several small molecule targets.[8] For example, FSA has been used recently to quantify opioids and/or their metabolites in urine at the pg/mL level[15] and to measure the protein biomarker, CYFRA 21.1 at ~60pg/mL which is nearly 10-fold more sensitive than electrochemiluminesence.[16] In particular, it has been illustrated that the aptamer-FSA-CIR method provides both highly sensitive quantification of opioids and their primary metabolites in urine, as well pharmacodynamics insights about these important molecules.[15]

Previous studies involving nucleotide double helix manipulation have further indicated that the magnitude of structural/conformational changes correlate with free- solution interferometric signal.[17] Capitalizing on the unique property that the FSA signal scales with changes in conformation and hydration, the research presented here investigates a method to potentially amplify the FreeSRF through rational design of the aptamer. This observation, combined with our recent FreeSRF modeling efforts led us to postulate that hairpin aptamers that unfold upon binding to a target and elicit a large conformational change would produce a large FSA response. To test

this hypothesis, we designed a series of hairpin aptamers with identical "loop" regions that bind the small molecule tenofovir, accompanied by a variable-length, self-associating stem region (**Figure 1)**.[18] Then the FSA binding response was measured as a function of stem-length. We demonstrate that the binding signal is inversely correlated with the number of self-associating base pairs in the aptamer stem region. Using this knowledge, we anticipate the potential to guide the aptamer design to improve the signal-to-noise ratio (S/N) for small-molecule aptamer-FSA assays.

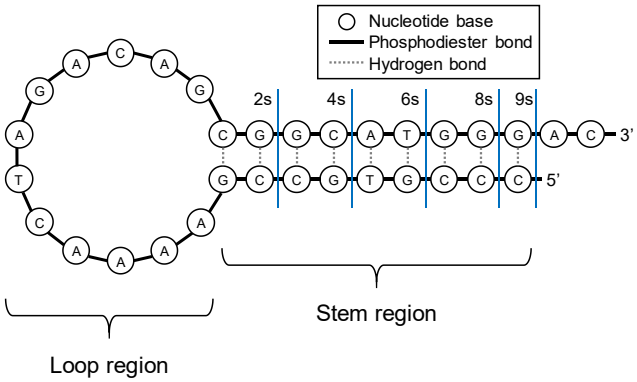


**Figure 1.** Hairpin aptamer showing the two regions of the structure: the loop region, which is constant across all structures, contains the binding region, and the stem region, which contains self-associating base pairs. The cutoff for each aptamer stem length is denoted by the blue line.

**Materials and Methods**

Single-strand DNA aptamers were selected by Base Pair Biotechnologies (Pearland, TX) using a modified SELEX process.[19] Tenofovir, phosphate buffered saline (PBS), sodium chloride, and magnesium chloride were obtained from Sigma Aldrich. All PBS used was modified to include 150 mM NaCl and 1 mM $MgCl_2$.

Prior to measurement by FSA, aptamers were refolded by incubation at 80°C for 5 minutes, then cooled to ambient temperature. All aptamers were screened against the small molecule target by incubating two concentrations of each aptamer (0 and 50 µM) with tenofovir (327.5 µM). For these screening experiments, we used very large concentrations of both the aptamer and the small molecule to ensure a robust signal. We used a relatively higher concentration of the small molecule (327.5 µM tenofovir versus 50 µM of the aptamer) to ensure all aptamer present in solution is bound despite differences in affinity between stem lengths. A blank consisting of tenofovir mixed with buffer was used to correct for the bulk RI. The only molecules present in the sample solutions are the aptamer, tenofovir, and phosphate buffered saline (used as purchased from Sigma-Aldrich). With nothing else present in solution, when there is no target present there should be no nonspecific interaction.

All binding affinity determinations were performed in an end-point format as previously described.[1b, 20] Briefly, a constant concentration of aptamer (1 nM) was incubated with increasing concentrations of tenofovir (0 to 40 nM). The concentration of aptamer was kept at or below the expected $K_D$ to ensure an accurate measurement of the $K_D$. The concentration of the aptamer was kept constant across the five different stem-lengths to obtain a more direct comparison for $B_{MAX}$. Reference samples were prepared by incubating the range of tenofovir concentrations with PBS, devoid of aptamer. Samples were incubated for 2 hours at 22°C before being measured using an interferometer in the sample-reference format described previously.[8] Measurements were made in triplicate. Dissociation constants ($K_D$) were determined by fitting the concentration dependent signal to a single site saturation isotherm (Y = X*Bmax / ($K_D$ + X)), where X is the concentration of analyte and Y is the instrument signal, using GraphPad Prism (GraphPad Software, Inc., La Jolla, CA).

Thermodynamic values were calculated using the mfold web server.[21] The free energies used are from the laboratory of John SantaLucia Jr,[22] and salt-correction was used with a 150 mM $Na^+$ and 1 mM $Mg^{2+}$ concentration, all other parameters were set to default. Aptamer 3D structures were simulated using RNA Composer.[23] The simulated 3D structures were used to perform ligand-docking simulations using Autodock VINA.[24]

**Results and Discussion**

**Figure 1** depicts the general structure for the hairpin aptamers developed for the small molecule tenofovir. This target was chosen because aptamers were available that assumed the hairpin shape and could be easily modified without altering the binding region. Furthermore, we have previously characterized the 9-stem aptamer by both BSI (9.0 nM) and MST (1.0 nM).[18] Additionally, cross reactivity measurements against a similarly-structured small molecule (ampicillin) were shown to elicit minimal off-target binding.[18]

Enabled by the mix-and-read FSA methodology and our compensated interferometer[8, 16] an end-point screening study was performed on aptamers with varying stem lengths (2, 4, 6, 8, and 9 base pairings, **Figure 1**). Here we use a fixed concentration of the small molecule target (327.5 µM of tenofovir) and hairpin aptamer (50 µM). **Figure 2A** illustrates that the binding signal of the five unique hairpin aptamers to tenofovir showed a 'decrease' in FSA signal as the length of the self-associating stem length was 'increased'. Interestingly, the aptamer with fewer self-associating stem base pairs (the "2-stem" aptamer) yielded the largest FSA signal (60 milliradians (mRad)), providing a ~6-fold signal increase over the aptamer with nine self-associating stem pairings (the "9-stem"). This observation confirmed our suspicion that 'a longer stem structure' does *not* necessarily lead to a larger FSA signal.

Further analysis of these observations are enlightening regarding the FSA mechanism. First, **Figure 2A** illustrates that the FSA signal exhibits a monotonic reduction in signal (slope of -7.5 ± 0.9 mrad/base pair, $R^2$ = 0.96) with increasing stem length. Second, this "inverse" relationship for stem length versus binding signal is not necessarily intuitive. One would assume more broken bonds and a larger conformation change would give a bigger FSA signal. Third, while conformation and hydration changes dominate the FSA signal,[3] here it appears that the prediction of the binding response of the hair-pin configuration requires the consideration of the need to overcome the energy for Watson-Crick pairing to break bonds in the stem distant from the loop. This energy boundary must be balanced by ability for the aptamer to form the target-probe complex, thereby undergoing structural and hydration changes. When paired bases in the hairpin are separated, the aptamer is allowed to unfold, presumably resulting in a subsequent increase the FreeSRF signal. Yet, as demonstrated below, there are other considerations when estimating the value of FreeSRF for aptamer-small molecule systems containing stem structures, including the 'strength' of the hairpin structure.

It has been previously shown that long hairpin tails can produce very stable structures, with 8-stem duplex species having up to picomolar binding affinities.[25] It is interesting that even the 9-stem tenofovir aptamer studied here gave $K_D$ measurements in the nanomolar range.[18]

This observation is likely attributable the fact that aptamer structures with longer stem regions are more likely to form stable complexes because they undergo base pair binding, making them less likely to dissociate. Yet, this observation may not apply to FSA measurements, which depends on conformational changes to report

the aptamer binding to the target. In other words, it is not necessarily expected that the interaction producing the highest affinity complex, would produce the largest FreeSRF signal. To test this hypothesis, we performed affinity determinations for each of the five aptamers binding to tenofovir. Taking into account that we started with the 9-stem aptamer and then snipped off stem sections prior to performing the binding experiments, the $K_D$ reported in this manuscript for the 9-stem aptamer corresponds quite well to that previously obtained and reported in our Analyst paper several years ago (~9nM in both cases for the 9-stem species). **Figure 2B** and **Table 1** present the results from these $K_D$ determinations, with a representative binding curve presented in **Figure 3**. The error in fitting the $K_D$ (**Figure 2B**) is a result of how well the line fits the data ($R^2$), but also the number and distribution of the analyzed data points (the measured ligand concentrations) and the error in replicate measurements for these samples. Much to our surprise, as we analyzed aptamers with *shorter length stems*, the measured binding affinities *increased* (a decrease in $K_D$) with stem length, implying a 'weaker' binding interaction between the aptamer and tenofovir. Interestingly, we also found that $B_{MAX}$ scaled inversely with the stem length. This observation is important, because for analyte quantification, the upper limit of the binding signal is bound by $B_{MAX}$. We hypothesize that aptamers with *fewer* stem region base pairings are more likely to dissociate upon binding the target than those with *more* base pairings, for small molecule – aptamer interactions. The larger FSA signal for shorter stems is somewhat counter intuitive and is presumably due to less structural rearrangement for the long stem probe being allowed.

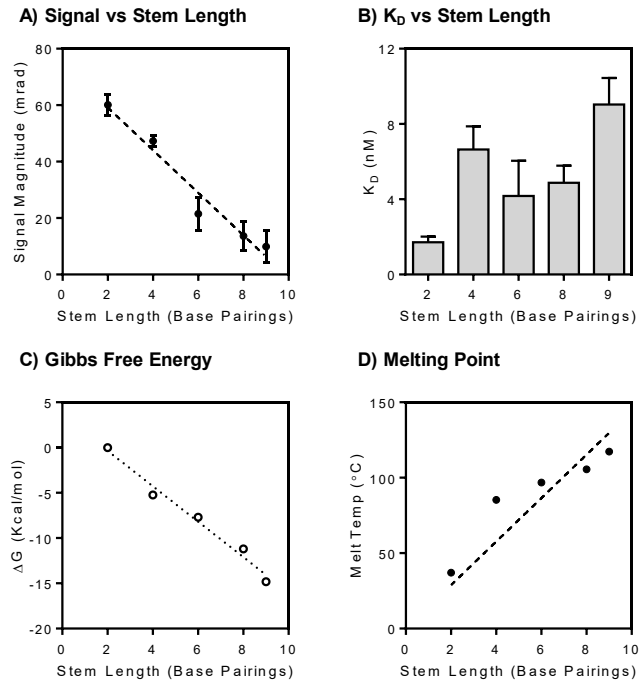


**Figure 2.** Tenofovir hairpin aptamers. Five hairpin aptamers with varying stem length bind to tenofovir with varying FSA signal magnitudes (A) and $K_D$ (B) despite identical target binding. A) Error bars represent standard deviation of 3 replicate trials. The dotted line is a fitted slope = -7.5 ± 0.9 mrad/base pair, $R^2 = 0.96$. B) $K_D$ fitted to single-site saturation isotherm (full data in Supporting Information figure S1). Error bars represent standard error of the fitted $K_D$. Thermodynamic calculations show a decrease in Gibbs free energy (C) and increase in melting temperature (D) correlating with increasing stem length.

**Table 1:** Affinity measurements and Thermodynamic values for the tenofovir aptamers

| *Stem Length* | *$K_D$ (nM)* | *$R^2$* | *$B_{MAX}$ (mrad)* | *Melting Temp (°C)* | *ΔG (kcal/mol)* |
|---|---|---|---|---|---|
| 2 | 1.71 | 0.991 | 44.2 | 37.1 | -0.01 |
| 4 | 6.64 | 0.980 | 30.2 | 85.3 | -5.23 |
| 6 | 4.17 | 0.888 | 18.1 | 96.8 | -7.7 |
| 8 | 4.88 | 0.980 | 10.1 | 105.5 | -11.2 |
| 9 | 9.04 | 0.988 | 15.3 | 117.3 | -14.82 |

To further unravel our observations we performed thermodynamic calculations of the Gibbs free energy (ΔG) and melting temperature ($T_m$) with stem-length of each aptamer using mfold® software (**Figures 2C-D**). **Figure 2C** illustrates that the 2-stem base pairing aptamer has a self-association ΔG of -0.01 kcal/mol, which means that the molecule has a very small energy barrier to overcome in order to *dissociate the stem*. Therefore the stem is easily forced apart upon binding to tenofovir. Meanwhile, the 9-stem aptamer exhibited a ΔG of -15 kcal/mol, meaning that self-association of the stem structure of the aptamer has an energy state that is considerably more thermodynamically favorable. In this case it would require substantially more energy to dissociate stem pairs. Remembering that in the free-solution assay, we start with the aptamer in the *associated* 'hairpin' form, and upon binding the small molecule the stem is presumably disrupted (or some portion of it) enabling binding of the probe to the target. This observation is important because it correlates with the general character of the ΔG plot that predicts the aptamer-tenofovir disassociation to be more favorable for short stem length aptamers.

The melting point of a DNA strand provides another metric for assessing the stability of a hybridization event.[26] Here we calculated $T_m$, finding that it increased with stem length. These observations provide further support for the hypothesis that fewer base pairings in the stem region are more likely to lead to dissociation upon binding. As such, an aptamer with a short stem, residing in a higher resting thermodynamic energy state, requires less energy to undergo a significant conformation change upon binding, resulting in a large FSA signal. Conversely, the aptamers with longer hairpins have a low ΔG and high $T_m$, making it energetically undesirable for the hairpin part of the probe to dissociate upon binding to tenofovir.

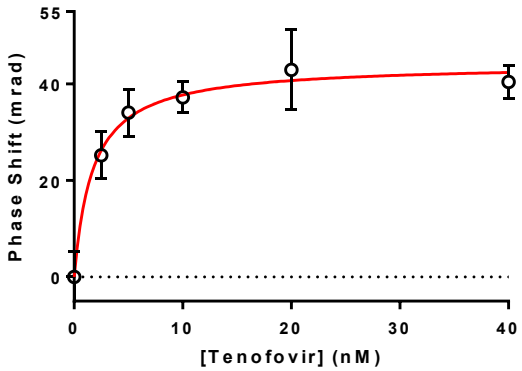


**Figure 3.** A representative binding curve of tenofovir binding to the aptamer, stem length 2 shown. Error bars represent the standard deviation of three independent trials.

In the case of longer stems, the target still binds to the probe, but with a reduced FSA signal and lower affinity (higher $K_D$). In this

case the longer stem aptamer likely binds to the target in the 'absence' of breaking some of the self-associating stem bonds, thus mitigating the magnitude of conformational / hydration change that would otherwise contribute to a larger FSA signal. This observation is also consistent with the FreeSRF model, which predicts that the binding signal magnitude scales with conformation and hydration changes.[3]

As shown in **Figure 4**, the results of Autodock VINA ligand docking simulations demonstrate the binding location is within the loop region of the aptamer. **Figure 4A** illustrates that when tenofovir binds to the 2-stem aptamer within the loop region it appears to place strain on the stem, presumably leading to a forced dissociation. In **Figure 4B** shows that tenofovir can potentially slip into the binding pocket without disturbing the stem region, largely because of the inherent stability of the multiple base-paired stem.

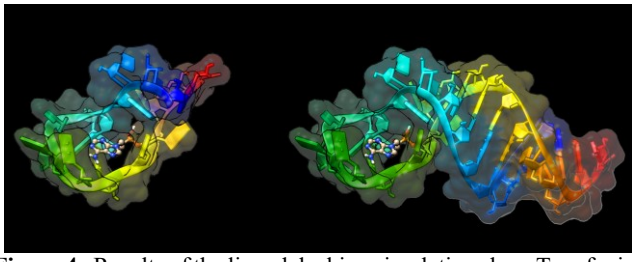

**Figure 4.** Results of the ligand docking simulation show Tenofovir binding to the "loop" region of the hairpin aptamer. A) Tenofovir binding to the 2-stem hairpin aptamer fits within the loop region and can easily force dissociation of the stem. B) Tenofovir binding the 9-stem hairpin aptamer can fit into the loop binding pocket without disturbing the stem region.

Collectively, we hypothesize that because the small molecule tenofovir binds in the loop region, there is reduced likelihood, or need, for the hairpin to *fully disassociate* during the binding event. It is probable that the stronger (longer) stems make it more difficult for the binding loop portion of the aptamer to make slight rearrangements necessary to let tenofovir slip into the pocket. Due to entropic drivers, it also appears that *shorter hairpins* dissociate more frequently, resulting in more binding events and a collectively larger conformational change, with the overall result of a larger FSA signal. In sort the tenofovir could bind inside the hairpin loop without adding enough stress to the stem region to force the longer stems apart.

In a report on the development of an ATP aptamer for the aim of exploring enantioselective sensor molecules for adenosine,[27] a temperature and stem-length dependency was observed for the fluorescently labeled aptamers. While interesting to note similar observations with other techniques, given the difference in the signal transduction mechanism (fluorescence versus structure and hydration changes), it is not clear to us that these observations provide additional insight into our stem-length observations. We hope to explore these potential insights in the future.

**Conclusion**

Hairpin aptamers likely undergo large conformational changes upon binding their target, and knowledge of the relative magnitude of these changes can enable optimization of the free-solution assay for a target. For a given aptamer, the obligate region for binding can be either the stem or the loop (or, less conveniently both) portion of the hairpin. Once the structure-activity relationship of the aptamer is minimally understood, rational design of the stem length can be used to obtain greater FSA signal upon binding, which can then be used to improve assay S/N and increase assay sensitivity/performance.

Here we observed that the FSA signal from small molecule binding hairpin aptamers is highest when the product results from easily dissociable hairpin bonds. For tenofovir, as the length of the hairpin is increased beyond favorable $\Delta G$ and $T_m$ conditions, the FSA signal magnitude degrades. Future work is focused on quantifying the binding affinity, specificity, limit of detection, and limit of quantification for hairpin aptamers to HIV p24, other proteins, and an array of small molecules, while implementing the findings presented here to aid in probe design to improve the sensitivity of quantitative assays.

## AUTHOR INFORMATION


**Corresponding Author**

**Darryl J. Bornhop** – *Department of Chemistry, Vanderbilt University, Nashville, TN 37235; Vanderbilt University Institute of Chemical Biology*; Phone: 615-322-4226; Email: darryl.bornhop@vanderbilt.edu

**Authors**

**Michael N. Kammer** – *Department of Chemistry, Vanderbilt University, Nashville, TN 37235*

**Amanda K. Kussrow** – *Department of Chemistry, Vanderbilt University, Nashville, TN 37235*

**Ian R. Olmsted** – *Department of Chemistry, Vanderbilt University, Nashville, TN 37235*

**George W. Jackson** – *Base Pair Biotechnologies, Inc. Pearland, TX 77584*


## ACKNOWLEDGMENT


This research was supported in part by a grant from the National Science Foundation (Grant CHE-1610964), and the Vanderbilt University Institute of Chemical Biology. GWJ is an employee of Base Pair Biotechnologies and has a financial interest in the tenofovir aptamers. DJB has a financial interest in Meru Biotechnologies, a company formed to commercialize FSA and the CIR. The other authors declare that they have no competing financial interests.


## SUPPORTING INFORMATION

Full saturation isotherms performed for all aptamers

## REFERENCES


1. (a) Bornhop, D. J.; Latham, J. C.; Kussrow, A.; Markov, D. A.; Jones, R. D.; Sorensen, H. S., Free-solution, label-free molecular interactions studied by back-scattering interferometry. *Science* **2007,** *317* (5845), 1732-1736; (b) Kussrow, A.; Enders, C. S.; Bornhop, D. J., Interferometric Methods for Label-Free Molecular Interaction Studies. *Anal Chem* **2012,** *84* (2), 779-792.
2. (a) Kammer, M. N.; Kussrow, A. K.; Olmsted, I. R.; Bornhop, D. J., A Highly Compensated Interferometer for Biochemical Analysis. *ACS Sensors* **2018,** *3* (8), 1546-1552; (b) Kammer, M. N.; Kussrow, A. K.; Bornhop, D. J., Longitudinal pixel averaging for improved compensation in backscattering interferometry. *Opt Lett* **2018,** *43* (3), 482-485.
3. Bornhop, D. J.; Kammer, M. N.; Kussrow, A.; Flowers, R. A.; Meiler, J., Origin and prediction of free-solution interaction studies performed label-free. *P Natl Acad Sci USA* **2016,** *113* (12), E1595-E1604.
4. Cho, E. J.; Lee, J. W.; Ellington, A. D., Applications of Aptamers as Sensors. *Annu Rev Anal Chem* **2009,** *2*, 241-264.
5. Kaur, G.; Roy, I., Therapeutic applications of aptamers. *Expert Opin Inv Drug* **2008,** *17* (1), 43-60.
6. Toulme, J. J.; Di Primo, C.; Boucard, D., Regulating eukaryotic gene expression with aptamers. *Febs Lett* **2004,** *567* (1), 55-62.
7. Cao, Z.; Tong, R.; Mishra, A.; Xu, W.; Wong, G. C.; Cheng, J.; Lu, Y., Reversible cell-specific drug delivery with aptamer-functionalized liposomes. *Angew Chem Int Ed Engl* **2009,** *48* (35), 6494-8.

8. Kammer, M.; Kussrow, A.; Carter, M. D.; Isenberg, S. L.; Johnson, R. C.; Batchelor, R. H.; Jackson, G. W.; Bornhop, D. J., Rapid quantification of two chemical nerve agent metabolites in serum. *Biosens Bioelectron* **2019,** *131*, 119-127.

9. Ruscito, A.; DeRosa, M. C., Small-Molecule Binding Aptamers: Selection Strategies, Characterization, and Applications. *Front Chem* **2016,** *4*.

10. (a) Aliakbarinodehi, N.; Jolly, P.; Bhalla, N.; Miodek, A.; De Micheli, G.; Estrela, P.; Carrara, S., Aptamer-based Field-Effect Biosensor for Tenofovir Detection. *Sci Rep-Uk* **2017,** *7*; (b) Vishnubhotla, R.; Ping, J. L.; Gao, Z. L.; Lee, A.; Saouaf, O.; Vrudhula, A.; Johnson, A. T. C., Scalable graphene aptasensors for drug quantification. *Aip Adv* **2017,** *7* (11); (c) Xiao, Y.; Lubin, A. A.; Heeger, A. J.; Plaxco, K. W., Label-free electronic detection of thrombin in blood serum by using an aptamer-based sensor. *Angew Chem Int Edit* **2005,** *44* (34), 5456-5459.

11. (a) Lee, J. H.; Wang, Z. D.; Liu, J. W.; Lu, Y., Highly Sensitive and Selective Colorimetric Sensors for Uranyl (UO22+) : Development and Comparison of Labeled and Label-Free DNAzyme-Gold Nanoparticle Systems. *J Am Chem Soc* **2008,** *130* (43), 14217-14226; (b) Peng, Y.; Li, L. D.; Mu, X. J.; Guo, L., Aptamer-gold nanoparticle-based colorimetric assay for the sensitive detection of thrombin. *Sensor Actuat B-Chem* **2013,** *177*, 818-825.

12. (a) Locke, A. K.; Norwood, N.; Marks, H. L.; Schechinger, M.; Jackson, G. W.; Graham, D.; Cote, G. L., Aptamer conjugated silver nanoparticles for the detection of interleukin 6. *Plasmonics in Biology and Medicine Xiii* **2016,** *9724*; (b) Marks, H.; Mabbott, S.; Huang, P. J.; Jackson, G. W.; Kameoka, J.; Graham, D.; Cote, G. L., Comparison of Fe2O3 and Fe2CoO4 core-shell plasmonic nanoparticles for aptamer mediated SERS assays. *Colloidal Nanoparticles for Biomedical Applications Xi* **2016,** *9722*; (c) Marks, H.; Mabbott, S.; Jackson, G. W.; Graham, D.; Cote, G. L., SERS active colloidal nanoparticles for the detection of small blood biomarkers using aptamers. *Colloidal Nanoparticles for Biomedical Applications X* **2015,** *9338*; (d) Marks, H. L.; Pishko, M. V.; Jackson, G. W.; Cote, G. L., Rational Design of a Bisphenol A Aptamer Selective Surface-Enhanced Raman Scattering Nanoprobe. *Anal Chem* **2014,** *86* (23), 11614-11619; (e) Walton, B. M.; Jackson, G. W.; Deutz, N.; Cote, G., Surface-enhanced Raman spectroscopy competitive binding biosensor development utilizing surface modification of silver nanocubes and a citrulline aptamer. *J Biomed Opt* **2017,** *22* (7).

13. (a) Gao, S. X.; Zheng, X.; Hu, B.; Sun, M. J.; Wu, J. H.; Jiao, B. H.; Wang, L. H., Enzyme-linked, aptamer-based, competitive biolayer interferometry biosensor for palytoxin. *Biosens Bioelectron* **2017,** *89*, 952-958; (b) Potty, A. S. R.; Kourentzi, K.; Fang, H.; Jackson, G. W.; Zhang, X.; Legge, G. B.; Willson, R. C., Biophysical Characterization of DNA Aptamer Interactions with Vascular Endothelial Growth Factor. *Biopolymers* **2009,** *91* (2), 145-156; (c) Wang, S.; Dong, Y. Y.; Liang, X. G., Development of a SPR aptasensor containing oriented aptamer for direct capture and detection of tetracycline in multiple honey samples. *Biosens Bioelectron* **2018,** *109*, 1-7.

14. (a) Falconer, R. J., Applications of isothermal titration calorimetry - the research and technical developments from 2011 to 2015. *Journal of Molecular Recognition* **2016,** *29* (10), 504-515; (b) Gaffarogullari, E. C.; Krause, A.; Balbo, J.; Herten, D. P.; Jaschke, A., Microscale thermophoresis provides insights into mechanism and thermodynamics of ribozyme catalysis. *Rna Biol* **2013,** *10* (12), 1815-1821.

15. Kammer, M. N.; Kussrow, A.; Gandhi, I.; Drabek, R.; Batchelor, R. H.; Jackson, G. W.; Bornhop, D. J., Quantification of Opioids in Urine Using an Aptamer-Based Free-Solution Assay. *Anal Chem* **2019,** *91* (16), 10582-10588.

16. Kammer, M. N.; Kussrow, A. K.; Webster, R. L.; Chen, H. D.; Hoeksema, M.; Christenson, R.; Massion, P. P.; Bornhop, D. J., Compensated Interferometry Measures of CYFRA 21-1 Improve Diagnosis of Lung Cancer. *Acs Comb Sci* **2019,** *21* (6), 465-472.

17. Adams, N. M.; Olmsted, I. R.; Haselton, F. R.; Bornhop, D. J.; Wright, D. W., The effect of hybridization-induced secondary structure alterations on RNA detection using backscattering interferometry. *Nucleic Acids Res* **2013,** *41* (9), e103.

18. Kammer, M. N.; Olmsted, I. R.; Kussrow, A. K.; Morris, M. J.; Jackson, G. W.; Bornhop, D. J., Characterizing aptamer small molecule interactions with backscattering interferometry. *Analyst* **2014,** *139* (22), 5879-5884.

19. Nutiu, R.; Li, Y. F., In vitro selection of structure-switching signaling aptamers. *Angew Chem Int Edit* **2005,** *44* (7), 1061-1065.

20. Olmsted, I. R.; Xiao, Y.; Cho, M.; Csordas, A. T.; Sheehan, J. H.; Meiler, J.; Soh, H. T.; Bornhop, D. J., Measurement of Aptamer-Protein Interactions with Back-Scattering Interferometry. *Anal Chem* **2011,** *83* (23), 8867-8870.

21. Zuker, M., Mfold web server for nucleic acid folding and hybridization prediction. *Nucleic Acids Res* **2003,** *31* (13), 3406-3415.

22. SantaLucia, J., A unified view of polymer, dumbbell, and oligonucleotide DNA nearest-neighbor thermodynamics. *P Natl Acad Sci USA* **1998,** *95* (4), 1460-1465.

23. Popenda, M.; Szachniuk, M.; Antczak, M.; Purzycka, K. J.; Lukasiak, P.; Bartol, N.; Blazewicz, J.; Adamiak, R. W., Automated 3D structure composition for large RNAs. *Nucleic Acids Res* **2012,** *40* (14).

24. Trott, O.; Olson, A. J., Software News and Update AutoDock Vina: Improving the Speed and Accuracy of Docking with a New Scoring Function, Efficient Optimization, and Multithreading. *J Comput Chem* **2010,** *31* (2), 455-461.

25. Armstrong, R. E.; Strouse, G. F., Rationally Manipulating Aptamer Binding Affinities in a Stem-Loop Molecular Beacon. *Bioconjugate Chem* **2014,** *25* (10), 1769-1776.

26. Ullman, J. S.; Mccarthy, B. J., Relationship between Mismatched Base Pairs and Thermal-Stability of DNA Duplexes .1. Effects of Depurination and Chain Scission. *Biochim Biophys Acta* **1973,** *294* (3), 405-415.

27. Urata, H.; Nomura, K.; Wada, S.; Akagi, M., Fluorescent-labeled single-strand ATP aptamer DNA: Chemo- and enantio-selectivity in sensing adenosine. *Biochem Bioph Res Co* **2007,** *360* (2), 459-463.

For Table of Contents Only